Southern
Illinois University
Carbondale

Lichang Wang
Associate Professor
Department of Chemistry and Biochemistry
Carbondale, IL 62901
Phone: 618-453-6476; FAX: 618-453-6408
E-Mail: lwang@chem.siu.edu
Web: http://www.chem.siu.edu/wang

Theoretical and Computational Chemistry —
Theory/Method/Software Developments and Applications

Progress Report

No. 2 August 2009

Research Perspective 3
Research Team 5
A. Theory/Method/Software Developments 7
- A1. Potential Energy Surface 7
- A2. Functional 8
- A3. Nuclear Density Functional Theory 8
- A4. Advanced Dynamics Simulation 9

B. Transition Metal Clusters and Nanoparticles 11
- B1. Structures and Electromagnetic Properties 11
- B2. Formation 11
- B3. Toxicity 12

C. Fuel Cells 15
- C1. Catalysis of Cathode Reaction 15
- C2. Catalysis of Hydrogen Production from Natural Gas 16

D. Clean Coal Utilization 17
- D1. Catalysis of Hydrogen/Methanol Production from Coal Gasification 17
- D2. Catalysis of Petroleum/Liquid-Fuel Production from Direct Coal Liquefaction 17
- D3. Solar Cell Materials 17

E. Solar Cells 19
- E1. Dye-Sensitized Solar Cells 19

F. Fluorescence Sensors 21
- F1. Metal Cation Sensors 21
- F2. pH Sensors 21
- F3. Organic Molecule Sensors 21

G. MASIS Center 23
- G1. Nanoparticle-Enhanced Chiral Recognition of Enantiomers 23
- G2. Boron Isotope Separation 23

Publications and Presentations 25
Support 28

Research Perspective

Driven by curiosity, passion, and expertise, research in Professor Wang's group at the Department of Chemistry and Biochemistry, Southern Illinois University Carbondale has been centered on developing theory/method/software and performing Computational Chemistry for studying chemical processes that take place in materials science and biological systems.

Our interest in theory/method/software developments includes constructing accurate potential energy surfaces for describing systems involving transition metals, formulating/implementing the NDFT (Nuclear Density Functional Theory) for describing dynamics of large systems full quantum mechanically, and coupling dynamics simulations with electronic calculations to monitor the change of electronic states during chemical reactions. Over the past three years, we have focused our efforts on building accurate potential energy surfaces for various transition metal clusters and nanoparticles, such as Ir_n, Pt_n, Au_n, and Ag_n, and performing comparative studies of different functionals in Density Functional Theory (DFT) calculations on systems of transition metal atoms.

Our interest in theory/method/software applications ranges from solving challenges in fuel cells, clean coal utilization, and solar cells to developing sensors. The underlying issues of our applications can be classified into three categories: chemical reactions including catalysis, photon-electron transfer processes, and chemical bonds, from covalent, ionic, to weak bonds. Over the past three years, we have looked into the catalysis of O_2 reduction, dehydrogenation of CH_4, and hydrogenation of hydrocarbons. We have studied adsorption/excitation of electrons in various organic dyes. Utilizing the change of interactions at different environments, we have been identifying/understanding better ways of separating boron isotopes and enantiomers, of detecting methane in air, and of forming hydrogen bonds among self-assembled organic layers.

Computational chemistry has been developed to the point that it can be used to greatly assist experimentalists to screen synthesis routes, to measure properties of materials that are difficult to perform under normal conditions, or to understand various mechanisms. Performing such tasks still relies on trained hands and minds. Thus, one of the goals in Computational Chemistry education is to create/provide ample opportunities for students to gain experiences on solving real problems. As such, we established the MASIS Center (Measurement And Synthesis In Silico Center). It is our hope that the MASIS center will help computational chemistry one step closer to become a tool that performs all the tasks in the synthesis of materials except for the final products and to replace the experimental measurements.

Research Team

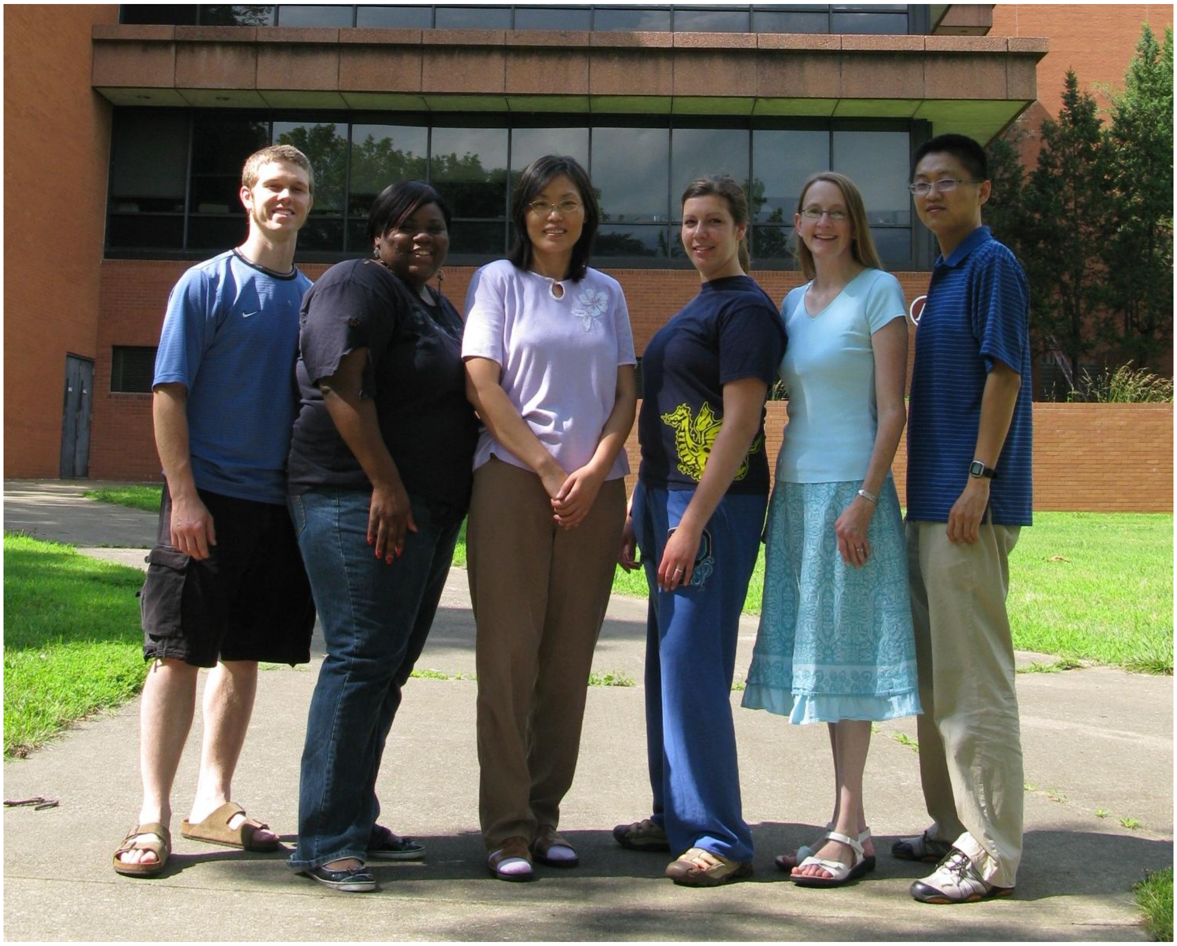

Current group members (Picture from left to right)

George Hudson (Ph.D student), **Chasity Love** (UG–Undergraduate Research Student), **Lichang Wang**, **Sarah Ferro** (UG), **Tiffany Pawluk** (Ph.D student), **Jianbo Li** (Ph.D student)

Past group members (since August 2006)

Tao Lin (Visiting Ph.D student), **Leah Bergquist** (2008 REU student), **Kasi Spivey** (M.Sc., May 2008), **Joe Williams** (UG)**, Brian Stachowiak** (UG), **Jennifer Yukna** (Ph.D, August 2007), **Mark Sadek** (UG), **Li Xiao** (Ph.D, May 2007)

Collaborators (since August 2006)

Prof. Minhua Zhang (Tianjin University)
Prof. Susan Lu (State University of New York at Binghamton)
Prof. Chang-jun Liu (Tianjin University)
Prof. Chuan-Jian Zhong (State University of New York at Binghamton)
Prof. Matthew E. McCarroll (SIUC–Southern Illinois University Carbondale)
Prof. Daniel J. Dyer (SIUC)

Progress A

Theory/Method/Software Developments

A1. Comparison and Construction of Potential Energy Surfaces for Describing Interactions among Atoms in Transition Metal Clusters and Nanoparticles [A1, A2]

Team members: Li Xiao, Tiffany Pawluk, Jennifer Yukna, Jianbo Li

Transition metal nanoparticles have been studied extensively due to their superior catalytic and optical properties over their bulk counterparts. One of the challenging issues facing the community is to synthesize well-controlled (in size and shape) nanoparticles. Understanding formation of transition metal clusters and nanoparticles is the first step towards this goal. Our approach is to perform Computational Chemistry, specifically dynamics simulations, to study the formation of various transition metal clusters (<1nm in size) and nanoparticles. Although ab intio molecular dynamics can provide insight into the formation of small clusters, dynamics simulations using potential energy surface will still be the working horse.

The most important input parameter in dynamics simulations is potential energy surface (PES). An accurate PES is essential to ensure the accuracy of results from these simulations. For transition metals, there are four types of PESs, i.e. the Finnis-Sinclair potentials, the embedded atom potentials, the tight binding potentials, and the Murrell-Mottram potentials, which have been widely used for describing interactions among transition metal atoms in bulk. When these PESs are used to describe interactions among atoms in nanoparticles, one question we asked is whether they are accurate. Our efforts towards answering this question started in Fall 2005. In the first effort, using Density Functional Theory (DFT) results of Ir_n, Pt_n, Au_n, Ag_n, we have examined the accuracy of the Sutton-Chen potential, which is a modified Finnis-Sinclair potential:

$$V = \varepsilon\left[\frac{1}{2}\sum_{ij} v(r_{ij}) - c\sum_{i}\sqrt{\rho_i}\right], \tag{1}$$

where the pair potential is given by

$$v(r_{ij}) = \left(\frac{a}{r_{ij}}\right)^n, \tag{2}$$

and the local electron density is given by

$$\rho_i = \sum_j \left(\frac{a}{r_{ij}}\right)^m. \tag{3}$$

In Eqs. (1)-(3), r_{ij} is the distance between two atoms and ε, a, c, m, and n are the parameters, which are constants for each metal but vary for different metals.

The parameters used in the original Sutton-Chen potential, denoted as the bulk Sutton-Chen potential, were optimized by fitting to the bulk properties of each metal. To investigate whether the Sutton-Chen potential can be used to accurately describe the interactions among transition metal atoms in clusters and nanoparticles, we used our DFT results for transition metal clusters as the "experimental" or fitting sets. The study shows that the original Sutton-Chen potential was not accurate for describing small metal clusters. We then optimized these parameters to the DFT results and constructed a new PES, cluster Sutton-Chen potential, for each of the Ir_n, Pt_n, Au_n, and Ag_n clusters.[A1]

Our fitting shows that the cluster Sutton-Chen potential still cannot predict the relative stability of isomers. We then turned our attention to use the artificial neural network (ANN) approach to construct PESs for these transition metal clusters and nanoparticles at the end of 2008. Three potential energy surfaces at the region of local minima for transition metal nanoparticles Pt, Au, and Ag, were derived using the artificial neural network method. Feedforward neural networks (FFNNs) with the modified back propagation algorithm were constructed to fit the complex relationship between the binding energy and the cluster size together with atomic coordinates (x_i, y_i, z_i). The inputs of those FFNNs are the number of atoms in each cluster and two variables derived from the distances between atoms within that cluster. Even though there is relatively small amount of data for both training and testing data of Pt, Au, and Ag systems, the artificial neural network approach still shows its capability for approximating the highly nonlinear relationship between input and output.[A2]

A2. Comparative Studies of Functionals in DFT Calculations [A3, A4]

Team members: Brian Stackowiak, Chasity Love, Sarah Ferro

One of our goals in the Theory/Method/Software developments is to assess the accuracy of various functionals that are widely used in the DFT studies associated with transition metal nanoparticles. Comparative studies have been carried out for Cu clusters using PW91, PBE, B3LYP, and M05 functionals since spring 2004.[A3] Since then, we have also compared the DFT results for the first and second row of transition metal dimers and trimers.[A4] Future work will include extending the comparative studies to other systems.

A3. Nuclear Density Functional Theory

For any given system, if the PES of the system is known, many interesting properties of the system can be obtained by solving nuclear equations of motion, i.e. the Schrödinger or the Newton equation. The most accurate description of dynamics for a system is the Schrödinger equation, but this can be done only for small systems, i.e. systems consisting of 4 or less atoms. For a system consisting of more than 4 atoms, the current practice is to describe its dynamics using either a pure classical method or an approximate method.

In the field of dynamics theory, two fundamental issues need to be addressed. One issue is that we don't yet have any measure of the accuracy of an approximate method when it is used to describe dynamics of a large system that shows a significant quantum character. The second issue is to develop a full quatum theory that can describe the dynamics of large systems within reasonable computational efforts. As such, since fall 2001, we have directed our efforts at providing solutions to these issues.

We have proposed a new full quantum dynamics theory, i.e. Nuclear Density Functional Theory (NDFT). Quite similar to the electronic DFT, the NDFT involves, in principle, solving the Kohn-Sham type equations for the nuclei in a homonuclear system:

$$[-\frac{1}{2\boldsymbol{M}}\nabla^2 + \boldsymbol{V}(\boldsymbol{R}) + \mu_c(\boldsymbol{R})]\psi_i(\boldsymbol{R}) - \int \frac{\rho(\boldsymbol{R},\boldsymbol{R}')}{|\boldsymbol{R}-\boldsymbol{R}'|}\psi_i(\boldsymbol{R}')\boldsymbol{dR}' = \varepsilon_i\psi_i(\boldsymbol{R}), \qquad (4)$$

$$\mu_c(\boldsymbol{R}) = \boldsymbol{d}(\rho\varepsilon_c)/\boldsymbol{d}\rho \quad \text{and} \quad \rho(\boldsymbol{R},\boldsymbol{R}') = \sum_{j=1}^{N}\psi_j(\boldsymbol{R})\psi_j^*(\boldsymbol{R}'), \qquad (5)$$

where these equations are the same as the electronic Kohn-Sham equations except for the variables V and R in the above equations representing the PES and the nuclear coordinates, respectively.

Despite the similarities in spirit between the electronic DFT and NDFT, there are many theoretical challenges need to be addressed before NDFT becomes a practical theory. For instance, the systems in the electronic DFT consist of only electrons. In contrast, NDFT will have to deal with systems with more than one type of nuclei. Therefore, a strategy has to be developed in NDFT to deal with systems consisting of different types of nuclei. One advantage of NDFT over the electronic DFT is that one can easily obtain accurate exchange-correlation energy. Preliminary framework of NDFT was developed, but many of the theoretical issues are being studied.

The implementation of the NDFT theory for systems consisting of the same type of atoms, i.e. uniatomic systems, is very similar to those of electronic DFT. However, for the systems consisting of more than one type of nuclei, different implementations will have to be employed. We are implementing the NDFT and using the dissociation of H_3^+ as our first benchmark system to test various perspective of the NDFT theory, though the work in this direction hasn't been progressed much since August 2006.

A4. Advanced Dynamics Simulations

Traditional molecular dynamics (MD) simulations provide us information on the dynamics aspects, such as rate constant, of catalytic processes of nanoparticles. However, the change of the electronic properties of these nanoparticles can only be probed by performing electronic structure calculations, such as DFT. Therefore, to have a complete picture of catalysis, we choose to couple the MD and DFT methods in our studies and denote it as the advanced molecular dynamics method (AMD). Since Spring 2007 we have built the first software, namely Coalescence, to study catalysis and formation of transition metal clusters/nanoparticles.

There are several ways to couple MD and DFT calculations. The most straightforward way is to perform MD simulations first and save the structural information, i.e. the Cartesian coordinates of each atom, at each time step. The DFT calculations can be performed consequently using these results. The time step in a typical MD simulation is in the range of 0.01-1 fs, and the simulation can run for ~10ps or longer. Therefore, the problem with this strategy is far too much data has to be saved. Additionally, too much computational time is needed. The alternative strategy, which we employed, is to carry out MD and DFT simultaneously. One of the advantages of this strategy is to be able to use the electronic wavefunctions generated from the past time step as the initial electronic wavefunction in the following DFT calculation. We are exploring other possibilities to reduce computing time. Further, the time between two DFT calculations will be set to a longer interval than 0.01 fs. A DFT calculation will be performed between two DFT calculations only when significant changes have taken place, which will be monitored in the MD simulations. We are testing extensively on how long the appropriate time interval will be and try to find an optimal choice and a common ground for different systems.

Abstracts:

[A1] **The impact of PES on MD results of the coalescence of M_2 + M with M = Ir, Pt, Au, Ag**
T. Pawluk, L. Xiao, J. Yukna, and L. Wang, *J. Chem. Theory Comput.* 3 (2007) 328-335.

The accuracy of the Sutton-Chen potential energy surface (PES) for describing atomic interactions in small metal clusters was investigated by comparison with density functional theory (DFT) calculation results. The binding energies calculated using the Sutton-Chen PES for the dimers, trimers, 8-, and 13-atom clusters of four transition metals, Ir, Pt, Au, and Ag differ from those obtained with DFT calculations. As the DFT results agree well with the available experimental data, the above disagreement indicates that the original Sutton-Chen PES cannot accurately describe the interactions among atoms in the cluster for these metals. The parameters of the Sutton-Chen potential were therefore optimized to the DFT results for each of the metals. Molecular dynamics (MD) simulations were carried out on the coalescence of a dimer with a single atom for these metals. Both the original bulk and the cluster optimized Sutton-Chen PESs were tested with various incident angles and initial kinetic energies. The MD results show that the coalescence is highly dependent on the PES. This demonstrates that use of an accurate PES is critical, particularly at low energy regime. The kinetic energy, incident angle, and choice of metal were examined for their role in the outcome of the coalescence process.

[A2] **Artificial neural network method to construct potential energy surfaces for transition metal nanoparticles: Pt, Au, and Ag**
Z. Xu, X. Shi, J. Li, S. Lu, and L. Wang, *IEEE proceeding of the 5th International Conference on Natural Computation* 1 (2009) 86-90.

Potential energy surfaces (PESs) for transition metal nanoparticles of Pt, Au, and Ag were derived using the artificial neural network (ANN) method. Three feedforward neural networks were constructed to fit the nonlinear relationship between the binding energy and the nanoparticle information, i.e. size and atomic coordinates, based on the data obtained from density functional theory calculations. The test results demonstrated that the newly derived ANN PESs can successfully predict the binding energy at the local minima of the global potential energy surfaces. More promisingly, the ANN PESs may be used in the molecular dynamics simulations for studying transition metal nanoparticles that are larger in size than those being studied here.

[A3] **Comparative density functional theory studies of Cu clusters**

C. B. Love, B. A. Stackowiak, and L. Wang, *Phys. Rev. B* (to be submitted).

The structures and electronic properties of small Cu clusters were studied using density functional theory (DFT) calculations. We present the results of DFT calculations for small Cu clusters up to fifty-five atoms. We chose to study linear, planar, and three-dimensional structures. Three functional, the Perdew-Wang 91 form of the generalized gradient approximation (PW91), Perdew-Burk-Ernzerhof functional (PBE), and Minnesota05 (M05) were used. We gathered the calculations of the binding energies, average bond lengths, magnetic moment, and the HOMO-LUMO gap of each cluster. Results showed that there was a transition from two-dimensional structures to three-dimensional structures being more stable at Cu_6, which agrees with other theoretical studies. As cluster size increase, there was monotonic decrease in magnetic moment for the odd number of clusters, while the magnetic moment for the even number of clusters was zero. It was also shown that as the linear cluster size increase, the bond distances between the atoms begin to alternate.

[A4] **Comparative DFT studies of transition metal dimers and trimers**

S. A. Ferro, C. B. Love, and L. Wang, *J. Chem. Theory Comput.* (to be submitted).

Understanding, and evaluating, the reliability of computational methods as they pertain to geometry optimization and frequency calculations of transition metal clusters is of great interest. In this work, calculations were performed using the Perdew-Burk-Ernzerhof (PBE) functional and the Lee-Yang-Parr correlation (B3LYP) functional on the dimers and trimers of the transition metals: Scandium, Titanium, Vanadium, Chromium, Manganese, Iron, Cobalt, Nickel, Copper, and Zinc. A plane wave basis set with cut-off energy of 300eV and LanL2DZ were used for PBE and LanL2DZ was used for B3LYP. The results include the binding energies, optimized geometries (bond lengths and bond angles), and frequencies. A comparison of PBE results with different basis sets and B3LYP results will be presented pertinent to the above listed transition metals. On average, B3LYP results yielded lower frequencies and lower binding energies than PBE results for identical clusters and metals.

Progress B

Transition Metal Clusters and Nanoparticles

B1. Structures and Electromagnetic Properties [B1-B6]

Team members: Li Xiao, Mark Sadek, Kasi Spivey, Brian Stackowiak, Chasity Love

Our research activities in the study of structures and electromagenetic properties of transition metal clusters and nanoparticles have focused on the studies of the size and structural effects on the energetic and electromagnetic properties of transition metal clusters/nanoparticles, Fe, Co, Ni, Cu, Ru, Rh, Pd, Ag, Os, Ir, Pt, Au, V, Mo, and their alloys, PtAu and PtVFe. The fundamental questions in the study of bare transition metal clusters include what are the most stable structures at a given size? Are there any novel structures other than the corresponding bulk structures? If yes, why do the most stable structures differ from the bulk structure? And how do various electromagnetic properties correlate with cluster size and structure?

The research focus in our previous progress report has been centered on to providing answers to the above questions. In the search for the most stable structure of small clusters, we found that *simple cubic structure* is the most stable structure among Ru, Ir, and Rh clusters consisting of more than 10 atoms. Our work also showed that a transition from the simple cubic to the corresponding bulk structure occurs at different cluster size depending on the element that it is made of. Furthermore, we predicted, based on our DFT calculations, that the transition from a more stable planar structure to a more stable three-dimensional structure for Au clusters occurs around the size of 13. Our DFT calculations also indicated the existence of single-walled Pd, Ir, and Pt nanotunes[B1] with interesting electromagnetic properties. Another class of novel structures predicted from our DFT calculations is transition metal fullerenes.

Since then, we have focused our attention to study the effect or the impact of ligands in the structure of clusters. Three ligands, i.e. SCH_3, HS, and CO, are emplyed in our DFT calculations. Using SCH_3 as ligands to explore the effect of ligands on the structure of Au_{11} clusters, we illustrated that the structures of small gold clusters can be altered substantially in the presence of ligands. In the case of Au_{11} clusters, the most stable structure is three-dimensional in the presence of SCH_3 ligands.[B2] The effect of CO on the structures of PtAu bimetallic clusters were also investigated.[B3,B4] We found that CO molecules can be adsorbed upside down, i.e. O bonds to the metal atom(s), in small PtAu clusters.[B4]

B2. Formation [B7, B8]

Team members: Tiffany Pawluk, Jennifer Yukna

Transition metal nanoparticles have been widely used as catalysts in many heterogeneous chemical reactions. Many fascinating properties exhibited by these nanomaterials are highly size and structure (or shape) dependent. For example, palladium clusters with less than 25 atoms have high catalytic activities for a number of reactions, but the catalytic activity varies with size. When highly active small nanoparticles aggregate to form large nanoparticles, a process termed as sintering in catalysis, the catalytic activities can be completely lost. As such, well-controlled synthesis of nanomaterials is imperative in the success of nanotechnology. After all, if no well-defined nanomaterials are synthesized, no sustainable applications of nanotechnology could be made.

Synthesis is clearly one of the permanent frontier areas in the process of discovery of new materials and technological advances. Different synthetic approaches often lead to different sizes and shapes (structures) of the final material. Therefore, the development of new techniques for synthesis and subsequent processing is vital for achieving materials with well controlled sizes and shapes. All too often, months or even years are spent developing synthetic techniques that can achieve the desired products. The ability to predict the synthetic route, before an expensive and time-consuming effort is undertaken, would dramatically improve the efficiency of synthesis.

While our long term goal is to develop the framework for computational synthesis of organic and inorganic materials, the current focus is on the synthesis of five types of clusters/nanoparticles, Pt, Au, Ag, Fe, and Ir. We are interested in understanding the formation mechanisms of small nanoparticles in the size range of less than 2 nm, obtaining the formation rate constant as a function of temperature, size, structure, and metal, and probing the evolution of the intrinsic electromagnetic properties of nanoparticles during formation process.

Transition metal nanoparticles have been synthesized in all three phases: gas phase, solution, and at the interface. The gas-phase preparation of metal clusters includes the formation of metal atoms by the decomposition of precursor gases, by sputtering or laser abalation. Our current simulation mimics gas phase synthesis. A question of fundamental importance is how properties and structures of small molecular clusters evolve into bulk materials. Although the stepwise growth of large transition metal clusters has been clearly elucidated, so far, no bulk material has been synthesized from an assembly of small well-defined molecular clusters that can clearly establish the direct relationships between the properties of the clusters and the bulk. The progress towards this goal has been slow, mainly because of the absence of unequivocal structural and mechanistic correlations between the solid-state phases and their relevant cluster derivatives.

The process of synthesis, or a cluster growth, can be divided into three stages. The first stage is nucleation. During the process of nucleation, upon collision of two species, the formation rate of a larger cluster depends critically on the means of heat removal. The second stage is cluster growth. The formation of a larger cluster in this stage is spontaneous. The excessive heat after collision affects the structure of the final product. The third stage is the termination of cluster growth. During this stage of growth, the two collision species are normally large in size themselves. The thermodynamic constraint of the systems makes the formation of an even larger cluster unfavorable, and therefore, the cluster growth becomes nonspontaneous.

Our approach is to perform dynamics simulations to study the formation of various transition metal clusters (<1nm in size) and nanoparticles. As transition metal atoms are heavy atoms, classical dynamics simulations are sufficient to describe the motions of these heavy atoms (more precisely, nuclei) using the coupled equations for position

$$\frac{dx_i}{dt} = \frac{p_{x_i}}{m_i}, \frac{dy_i}{dt} = \frac{p_{y_i}}{m_i}, \frac{dz_i}{dt} = \frac{p_{z_i}}{m_i}, \tag{6}$$

and momentum

$$\frac{dp_{x_i}}{dt} = -\frac{\partial V}{\partial x_i}, \frac{dp_{y_i}}{dt} = -\frac{\partial V}{\partial y_i}, \frac{dp_{z_i}}{dt} = -\frac{\partial V}{\partial z_i}, \tag{7}$$

in the Cartesian coordinates x, y, and z for each atom, *i*, where m_i is the mass of the *i*t atom, and V is the PES.

Over the past three years, we have studied the coalescence of Ir[B7] and Ag clusters.[B8] The size of our systems are within the range of second stage of cluster growth.

B3. Toxicity

Transition metal nanoparticles are among the most potentially useful nanomaterials as catalysts and in biotechnology. These nanomaterials, not surprisingly, have been studied over the past decades by many groups including ours. Their medical use as imaging reagents has a direct impact on a range of health-related issues. These nanoparticles, as catalysts or coating materials, can also enter human bodies by inhaling or other means. However, the toxicity of these nanoparticles is not fully understood. For instance, silver is generally low in toxicity, silver nanoparticles (widely known as nano-silver) is considered to be toxic. This indicates that their toxicity cannot be derived from the original materials. The lack of rigorous toxicity studies of transition metal nanoparticles makes them prone to catastrophic failure in their potentially important applications. Our research aims to establish quantitative structure-activity relationships for nano-silver through computational studies. Specifically, we use DFT calculations to study the binding properties of silver nanoparticles to Transferrin (Tf), Human hepatocellular carcinoma (HepG2), and gramicidin A channel. These calculations will be used to predict various binding sites and to obtain binding energies and frequency shifts of key functional groups. There are two key elements to our DFT studies. First, the interaction (or binding) will be studied at different levels with increasing size: unit, segment, domain, and entire system. Our hypothesis is that most binding will be local in character. Second, a protocol to define the proper size for binding study will be developed based on these systematic studies.

We also use MD simulations to study the behavior of HepG2 cells in the presence of silver nanoparticles. The simulation results will reveal the early stage of how silver nanoparticles induce biophysical changes to the cellular membrane. This study will provide an insight into how silver nanoparticles, possibly other transition metal nanoparticles, enter human cells and the roles they play in human toxicology.

Cytotoxicity is usually measured by the MTT (dimethyltriazoldiphenyl tetrazolium-formazan) assay, Trypan blue assay, Sulforhodamine B assay, and clonogenic assay, however, no quantities at atomic/molecular level are yet defined to measure the cytotoxicity. Through analysis of the combined DFT and MD results, we attempt to search for the quantities that can be used to describe the characteristics of toxicity at atomic/molecular level while can also be measured experimentally in toxicity studies of Nano-silver and other transition metal nanoparticles. This objective evaluates the feasibility of using computations as driving force in toxicity studies of transition metal nanoparticles.

Abstracts:

[B1] **Density functional theory study of single-wall platinum nanotubes**

L. Xiao and L. Wang, *Chem. Phys. Lett.* 430 (2006) 319-322.

Single-wall platinum nanotubes (SWPtN) were studied using spin-polarized density functional theory calculations. These nanotubes consist of 5-, 6-, and 8- Pt atoms coiling around the tubular axis forming 3.54–4.73 Å in diameter and 0.7–1.4 nm and infinite in length. Two types of wall structures, square and triangular, were investigated. The results show that triangular nanotubes are more stable. Our results suggest that it is also feasible to synthesize the 5- and 8-atom triangular nanotubes as the 6-atom Pt nanotubes were found experimentally. These SWPtN may provide a new dimension in the catalytic applications of platinum.

[B2] **Structures of undecagold clusters: Ligand effect**

K. Spivey, J. I. Williams, and L. Wang, *Chem. Phys. Lett.* 432 (2006) 163-166.

The most stable structure of undecagold, or Au_{11}, clusters was predicted from our DFT calculations to be planar [Chem. Phys. Lett. 392 (2004) 452; J. Chem. Phys. 124 (2005) 114309]. The structures of ligand protected undecagold clusters were shown to be three-dimensional experimentally. In this work, we used DFT calculations to study the ligand effect on the structures of Au_{11} clusters. Our results show that the most stable structure of Au_{11} is in fact three-dimensional when SCH_3 ligands are attached. This indicates that the structures of small gold clusters are altered substantially in the presence of ligands.

[B3] **Effect of adsorption site, size, and composition of Pt/Au bimetallic clusters on the CO frequency: A density functional theory study**

M. M. Sadek and L. Wang, *J. Phys. Chem. A* 110 (2006) 14036-14042.

Density functional theory (DFT) calculations were performed to investigating the C–O stretching frequency changes when CO molecule was adsorbed to the Pt/Au clusters of 2-4 atoms. Our calculations show that the adsorption site is the most sensitive quantity to the C–O stretching frequency shifts. All the bridge site adsorptions yield a CO frequency band of 1737–1927 cm^{-1} with the CO bond distance of 1.167–1.204 Å regardless cluster composition and size, and all the atop site adsorptions yield a CO frequency band of 2000–2091 cm^{-1} with the CO bond distance of 1.151–1.167 Å. More detailed analysis of the two frequency bands shows that each band may consist of two emerging subbands with the lower frequencies corresponding to the CO adsorption to Pt atoms and the higher frequencies to the CO adsorption to Au atoms. Furthermore, the CO frequency decreases with increasing Pt composition in the bimetallic clusters. Our results indicate that the Fourier transform infrared spectroscopy measurement may be used as a sensitive tool to identify adsorption sites and perhaps surface composition of the Pt /Au nanoparticles using CO adsorption as the probe.

[B4] **CO adsorbs upside-down on small Pt_mAu_n clusters**
L. Wang, *Chem. Phys. Lett.* 443 (2007) 304-308.

Density functional theory calculations were carried out for CO upside-down adsorption, namely the O atom close to the metal atom, on small Pt_mAu_n clusters (m, n = 0–4) and on Pt(111), Au(111), and $Pt_{0.25}Au_{0.75}(111)$ surfaces. The results show that CO can adsorb upside-down on the clusters but not on the bulk surfaces. Analysis combining both the adsorption energy and CO stretching frequency data indicates that the CO upside-down adsorption on pure Pt clusters may be detected experimentally using FTIR spectroscopy alone while those on pure Au and Pt_mAu_n clusters may be detected using FTIR coupled with TPD techniques.

[B5] **Theoretical studies of silver clusters**
J. Yukna, H. Tang, J. Li, and L. Wang, *Phys. Rev. B* (submitted).

Silver clusters consisting of 2-55 atoms were investigated using spin polarized density functional theory calculations with PW91 functional and a plane wave basis set. Linear clusters were found to undergo Peierls bond distortion and the most stable planar clusters have high coordination numbers. The results show that planar silver clusters up to six atoms are more stable than their three-dimensional isomers. The linear trimer is just as stable as the planar trimer. New global minima were found for clusters of 9, 10, and 13–20 atoms. The most stable even numbered clusters are singlet and odd-numbered clusters are doublet. The Sutton-Chen potential was also used to calculate the relative stability of selected clusters; however, the results overestimate the binding energy of these clusters. This suggests that a modification has to be made in order to use it in the search of global minima for larger silver clusters or in the study of coalescence of silver clusters. In this work, the Sutton-Chen potential was modified by fitting the Sutton-Chen parameters to the selected DFT results. The modified Sutton-Chen potential agreed well with the DFT results.

[B6] **Comparative density functional theory studies of Cu clusters** (also listed previously as [A3])
C. B. Love, B. A. Stackowiak, and L. Wang, *Phys. Rev. B* (to be submitted).

[B7] **Molecular Dynamics Simulations of the Coalescence of Iridium Clusters**
T. Pawluk and L. Wang, *J. Phys. Chem. C* 111 (2007) 6713-6719.

The coalescence of small iridium clusters was studied using a molecular dynamics (MD) technique with a cluster Sutton-Chen potential. MD simulations were carried out on the reaction of two clusters from 1 to 7 atoms at various incident angles and initial kinetic energies. The threshold energy of product formation was investigated for the various systems, and the effect of initial orientation between two clusters on the product was also studied. A comparison of diffusion and Ostwald-ripening coalescence mechanisms was performed for 8-atom cluster formation, and Ostwald-ripening led to cluster formation with higher initial energies. An atom-to-bond collision resulted in the formation of a larger cluster more often and at higher energies than an atom-to-atom collision.

[B8] **Molecular Dynamics Studies of the Coalescence of Silver Clusters**
J. Yukna and L. Wang, *J. Phys. Chem. C* 111 (2007) 13337-13347.

The coalescence of two silver clusters was studied using molecular dynamics simulations governed by the cluster Sutton-Chen potential. These simulations were carried out for 10 systems with the silver clusters consisting of 2-8 and 19 atoms colliding at different kinetic energies and initial orientations. The products are mostly nonreactive product for Ag_2 + Ag and $Ag_n + Ag_n$ with n = 2-4. This indicates that the nucleation is dominant in the coalescence of the systems consisting of 8 or less Ag atoms. The studies of $Ag_n + Ag_n$ with n = 7, 8, and 19 revealed that the coalescence product, i.e., Ag_{2n}, forms at all cases. This illustrates that the cluster growth is dominant in the coalescence of the systems consisting of 14 or more Ag atoms.

Progress C

Fuel Cells

C1. Catalysis of Cathode Reaction—O_2 reduction [C1]

Team members: Joe Williams, Tao Lin

An important issue in the design of hydrogen fuel cell is the lack of efficient cathode catalysts for oxygen reduction that can operate at room temperatures. Common cathode catalysts are platinum or platinum based alloys. It has been shown experimentally that bimetallic or ternary platinum alloys are more efficient catalysts. Theoretical studies of alloy catalysts will be helpful in understanding of their catalytic activities and consequently be helpful in the practical design. In addition, platinum is expensive and its replacement will be economically useful. The purpose of our research in the study of oxygen reduction is, therefore, two folds. One is to understand why platinum alloys have better catalytic activities. The second is to explore what is the minimum Pt composition such that the alloys still maintain high catalytic activities. Towards that end, DFT calculations were performed for O_2 chemisorptions, molecular and dissociative, in the presence of PtVFe, Pt_3, and $PtFe_2$. It has been found that PtVFe is a better catalyst in O_2 chemisorption due to higher charge transfer to O_2, direct dissociative pathways, and narrower barrier widths. In the case of indirect pathway, a comparison between PtVFe and Pt catalysts, is shown in the Figure below.[C1]

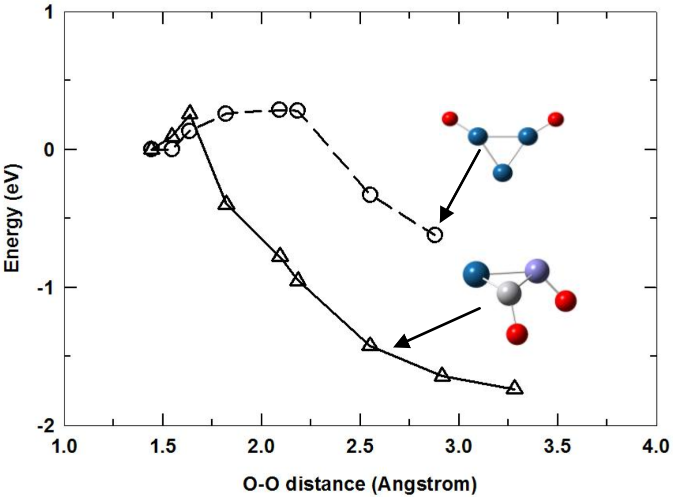

A comparison of energy profiles for two reaction pathways for O_2 dissociation on PtVFe (solid line with triangles) and Pt_3 (dash line with circles).

The rate constant, *k*, was calculated using the harmonic transition state theory expressed as,

$$k = \frac{\prod_i^{3N} \nu_i}{\prod_i^{3N-1} \nu_i^{\neq}} e^{-\Delta E / k_B T}, \qquad (8)$$

where ν_i and $\nu_i^{\neq}$ are the frequencies of reactant and transition state, respectively. The reaction barrier height, ΔE, is 0.26 eV for the PtVFe trimer and 0.29 eV for the Pt_3 with the reaction pathways depicted in the left Figure. k_B and T is the Boltzmann constant and temperature, respectively. Table below shows the reaction rate constant as a function of temperature obtained using the above Equation for O_2 dissociation on the model catalysts, PtVFe and Pt_3 trimers in the case of indirect dissociation.

The O_2 dissociation rate constant as a function of temperature for the reactions shown in the Figure above.

T (^{o}C)	k_1 (PtVFe), s^{-1}	k_2 (Pt_3), s^{-1}	k_1/k_2
25	4.29×10^{9}	9.71×10^{8}	4.4
50	9.39×10^{9}	2.32×10^{9}	4.0
75	1.84×10^{10}	4.91×10^{9}	3.7
100	3.28×10^{10}	9.39×10^{9}	3.5
125	5.45×10^{10}	1.65×10^{10}	3.3

C2. Catalysis of Hydrogen Production from Natural Gas [C2, C3]

Team members: Li Xiao, Tiffany Pawluk

Dehydrogenation of methane to produce H_2 is an interesting route to provide fuel for hydrogen fuel cells. In this work, we studied the catalytic process of CH_4 dehydrogenation in the presence of Pt and Ir.

Methane activation on Pt surfaces and clusters has been studied extensively both experimentally and computationally due to the practical applications. However, to fully understand methane activation on transition metal nanoparticles, further investigation in both experiments and computation is needed. For instance, theoretical studies of CH_4 activation on Pt clusters were done only for systems consisting of 1-2 Pt atoms. We carried out DFT studies of CH_4 activation on one Pt atom and Pt_4 cluster. Both B3LYP and PW91 were used in our study. New lower energy reaction pathway was obtained for CH_4 activation in the presence of one Pt atom. Reaction pathways were also obtained for the first time for CH_4 activation in the presence of a 4-atom Pt cluster. Furthermore, our study shows that the most discrepancies between the B3LYP and PW91 results are in the calculation of reaction barrier height.[C2] In the case of Ir, an easier, or barrierless, pathway is located.[C3]

Abstracts:

[C1] **Optimal Composition of Ternary Nanoparticle Catalysts for Oxygen Reduction Reaction**
L. Wang, T. Lin, J. I. Williams, J. Luo, P. N. Njoki, D. Mott, R. Loukrakpam, C.-J. Zhong, *J. Am. Chem. Soc.* (submitted).

An integrated computational and experimental approach was developed to determine the optimal compositions of ternary nanoparticles for catalyzing oxygen reduction reaction. For PtVFe nanoparticles, the composition of ~33% Pt, ~15% V, and ~52% Fe was shown to achieve the optimal electrocatalytic activity. Density functional theory calculations reveal that the enhanced activity of PtVFe nanoparticles, four times as active as Pt and twice as PtFe, is due to (1) the direct or spontaneous O_2 dissociations in comparison to pure Pt nanoparticles and (2) efficient electron transfer in the presence of V.

[C2] **Methane activation on Pt and Pt_4: A density functional theory study**
L. Xiao and L. Wang, *J. Phys. Chem. B* 111 (2007) 1657-1663.

The activation mechanisms of a methane molecule on a Pt atom (CH_4-Pt) and on a Pt tetramer (CH_4-Pt4) were investigated using density functional theory (B3LYP and PW91) calculations. The results from these two functionals are different mostly in predicting the reaction barrier, in particular for the CH_4-Pt system. A new lower energy pathway was identified for the CH_4 dehydrogenation on a Pt atom. In the new pathway, the $PtCH_2 + H_2$ products were formed via a transition state, in which the Pt atom forms a complex with carbene and both dissociated hydrogen atoms. We report here the first theoretical study of methane activation on a Pt_4 cluster. Among the five single steps toward dehydrogenation, our results show that the rate-limiting step is the third step, that is, breaking the second C-H bond, which requires overcoming an energy barrier of 28 kcal/mol. On the other hand, the cleavage of the first C-H bond, that is, the first reaction step, requires overcoming an energy barrier of 4 kcal/mol.

[C3] **Studies of Ir catalyzed CH_4 dehydrogenation using PBE, PW91, and B3LYP functional**
T. Pawluk and L. Wang, *Phys. Chem. Chem. Phys.* (to be submitted).

Methane dehydrogenation in the presence of a single iridium atom was studied by DFT using PW91, PBE, and B3LYP. A new, lower energy reaction pathway was located for the dehydrogenation reaction on a single Ir atom. Although the ground state of Ir is quartet, the reaction involves a spin-switching from quartet to doublet after formation of an $IrCH_4$ adduct, requiring 7 kcal/mol to overcome the energy barrier with respect to the quartet reaction asymptote. This energy barrier is significantly lower than for Pt. The doublet reaction pathway is favored for the remainder of the reaction. All intermediates and transition states along the doublet surface are below the doublet reaction asymptote; the dehydrogenation reaction along this doublet surface is barrierless.

Progress D

Clean Coal Utilizations

D1. Catalysis of Hydrogen/Methanol Production from Coal Gasification

Team members: Chasity Love

Our computational studies of the feasibility of a new pathway for hydrogen/methanol production from coal gasification involve the use of the-state-of-the-art first principles calculations. We proposed a new reaction pathway that reduces the consumption of hydrogen generated in the gasification and replaces CH_4 with a more manageable product, CH_3OH.

The feasibility of such a pathway depends on whether we can develop catalysts that favor CH_3OH formation but eliminate CH_4 formation. To achieve this, we need a better understanding of reaction mechanisms at an atomic level and screen various potential catalyst candidates which are active towards these reactions. As such, we performed DFT calculations for a selection of catalyst candidates. We started by examining the catalysts for methanol synthesis, such as the leading industrial catalyst Cu/ZnO. We then focus on studies of the role of Cu/ZnO in elementary reactions such as CH_3OH and CH_4 formation as well as H_2O dissociation, the most critical reaction steps in the newly proposed coal gasification pathway. Our previous study shows that Cu surface is not very active towards H_2 dissociation. Furthermore, an adsorbed CH_3 on an extended surface may pose significant steric hindering for further reaction. On the other hand, Cu clusters with corners and edges may be active catalysts. Therefore, we studied Cu clusters supported by ZnO. We are to study the interactions between CH_3, H, OH, H_2O, CH_4, CH_3OH, and Cu/ZnO at different Cu sites, the energetics of coadsorption of CH_3 and H on Cu/ZnO and of CH_3 and OH on Cu/ZnO, then to search for the reaction path leading to the dissociation of H_2O and the formation of CH_4 and CH_3OH on the Cu/ZnO catalysts. This will lead us to be able to screen the binding sites on Cu/ZnO and search for the conditions that maximize CH_3OH formation.

D2. Catalysis of Petroleum/Liquid-Fuel Production from Direct Coal Liquefaction

Our work in direct coal liquefaction (DCL) of Illinois coal is centered on searching for optimal catalysts that can take advantage of the high sulfur content of Illinois coal and reduce the capital investment and operational cost of the DCL technology. Selection of optimal catalysts depends critically on the understanding of the properties of catalysts and the mechanisms of catalytic reactions. Consequently, our research activities focus on the understanding of catalytic activities of Fe and Mo-doped Fe nanocatalysts and on establishing the correlation between the properties of the nanocatalysts and their catalytic activities through employing the cutting-edge integrated approach, in which computational studies are carried out to provide the strategic guidance on the actual synthesis of catalysts. Specifically, we focus on using DFT and molecular dynamics simulations to obtain the properties of the nanocatalysts and study their catalytic activities in hydrogenation, i.e. breaking the C=C and C-C bonds with addition of H atoms, of model Illinois coal: sulfur-containing benzene ($C_6H_5SCH_3$) and naththalene ($C_{14}H_9SCH_3$).

D3. Coal as Solar Cell Materials

The development goal of solar cells is to convert solar energy to electricity at the cost of ~2cents/kWh ($0.40/W). As shown in the Figure next page (took from Basic Research Needs for Solar Energy Utilization, DOE 2005), the area marked in red is the direction that research is heading. Under this strategy, a drastic increase of conversion efficiency has to be achieved. Another strategy, labeled in blue in the Figure, illustrates our way of approaching the development goal: reducing the cost of materials while mildly improving the conversion efficiency. Note that the green and pink marked areas correspond to the bulk Si and thin film dye-sensitized organic solar cells, respectively.

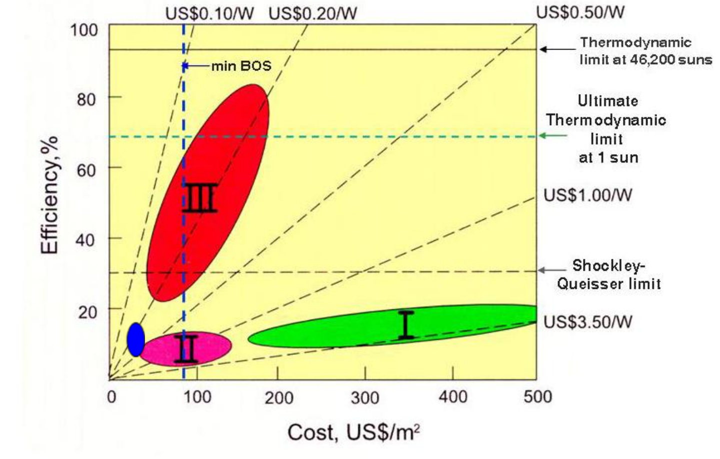

For PV or PEC to provide the full level of C-free energy required for electricity and fuel—solar power cost needs to be ~2 cents/kWh ($0.40/W$_p$).

Conversion of solar energy to the energy can be made through different pathways. The most common ones are (1) photothermal (PT) process, i.e. converting solar energy to thermal energy, (2) Photovoltaic (PV) process, i.e. converting solar energy to electricity, (3) Solarchemical (PC), converting solar energy to chemical energy. In our approach, we aim to use photovoltaicthermal (PVT) process to capture solar energy simultaneously in electricity and thermal energy. In this research, we explore the utilization of coal as such materials to convert solar energy to electricity and thermal energy.

As coal is a mixer of compounds, we are examining various structures of coal in their role and feasibility on transferring electrons upon absorption of solar energy and converting to thermal energy.

Progress E

Solar Cells

E1. Dye-Sensitized Solar Cells [E1]

Team members: George Hudson

The Basic Energy Sciences (BES) of DOE workshop report on solar energy utilization stated that a grand challenge for photovoltaics is the development of high-efficiency, low-cost photovoltaic structures that can reach the ultimate thermodynamic efficiency limits, shown in the Figure below (taken from www.er.doe.gov/bes/reports/files/SEU_rpt.pdf). Several techniques exist toward the realization of photovoltaic devices with efficiency greater than 50%, such as multiple junction solar cells (tandems), optical frequency shifting solar cells, multiple energy level solar cells, and hot carrier solar cells.

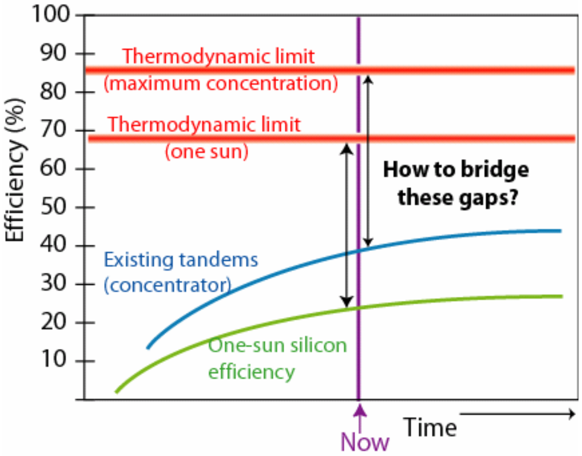

Understanding photon-induced electron and charge transfer mechanisms in solar cells is the key step towards bridging the efficiency gap. Charge recombination is generally considered to be an important factor responsible for the low efficiency of organic dyes. Different design strategies to preventing charge recombination have been developed over the traditional organic and organometallic donor-acceptor compounds. However, little is studied on the possibility and consequence of competitive or simultaneous photon-induced multiple electron and charge transfer processes with each electron excitation takes place at different moieties of a dye compound. The broad solar spectrum can certainly accomplish such simultaneous multiple electron excitations. Our preliminary results show that two photons of different energies can indeed excite electrons in different moieties of Compound 1 (Figure 1). We aim to study multiple-electron and charge transfer dynamics in organic dyes to provide insight into the electron transfer mechanisms of organic dyes in solar cells.

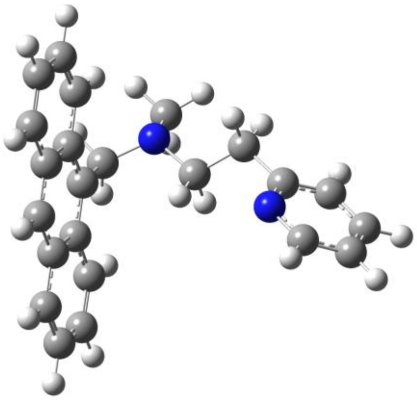

Fig. 1 Compound 1. The blue, grey, and white balls represent nitrogen, carbon, and hydrogen atoms, respectively.

The time-dependent density functional theory calculations (TDDFT) were performed and the relevant molecular orbitals are depicted in Fig. 2. The TDDFT results predict that two electrons can be excited simultaneously. One is from MO84—MO89 with excitation energy of 234 nm and another is MO87→MO88 with excitation energy of 401 nm. In the proposed research, we will perform kinetics studies for this compound and study how the excited electrons travel from their corresponding moiety to another, and whether/how these processes interfere each other.

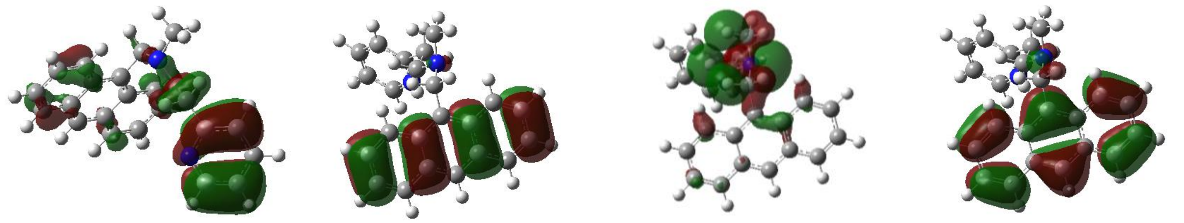

MO84 (-7.12 eV) **MO85 (-6.79 eV)** **MO86 (-6.01 eV)** **MO87 (-5.51 eV) (HOMO)**

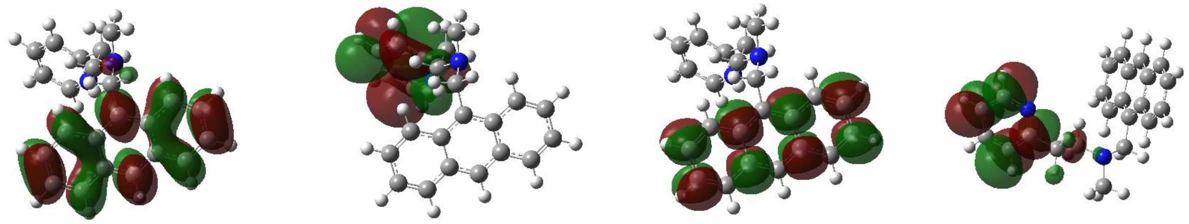

MO88 (-2.04 eV) (LUMO) **MO89 (-1.02 eV)** **MO90 (-0.74 eV)** **MO91 (-0.64 eV)**

Figure 2. Molecular orbitals (MO's) of Compound 1.

The second system (including three compounds) has been studied is shown on the right. These compounds were synthesized as organic dyes for solar cells. Both electronic and kinetics calculations will be performed for these compounds.

One of our goals is to find ways to allow the dye to absorb lights in the visible region. Our work along this direction is shown in publication [E1].

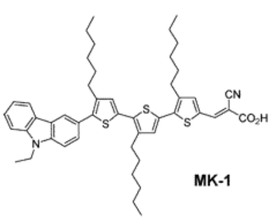

MK-1

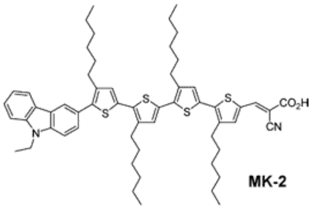

MK-2

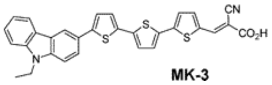

MK-3

Abstracts:

[E1] **A silole substituted carbazole dye for dye-sensitized solar cells: A computational study**
G. A. Hudson and L. Wang, *Chem. Phys. Lett.* (to be submitted).

Substituting a thiophene ring in the MK-3 dye with a silole ring, the B3LYP and TD-B3LYP calculations have shown that the adsorption of photons of the new dye, Me_2Si-MK-3, is red-shifted to longer wavelength. The red shift is due to a higher energy HOMO in the Me_2Si-MK-3 dye (-4.992 eV) compared to the MK-3 dye (-5.153 eV). Furthermore, the substitution resulted in a slight distortion of the π-π conjugation. Both higher HOMO level and the breaking of π-π conjugation help preventing the charge recombination, and thus increasing the efficiency of the DSSCs.

Progress F

Fluorescence Sensors

F1. Metal Cation Sensors [F1, F2]

The goal of this research project, as well as other sensor projects described below, is to guide the design of fluorescence sensors with satisfactory sensitivity and selectivity using various theoretical tools. The transduction mechanism of our fluorescence sensors is based on Photoinduced Electron Transfer (PET) through molecular recognition events. A typical fluorescence sensor (see the flow chart below) consists of three components, i.e. a fluorophore, a spacer, and a receptor with a recognition site or binding site to bind analytes.

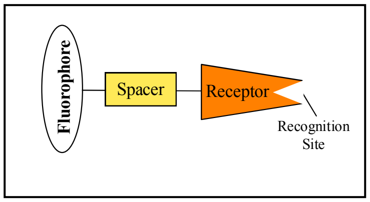

The “On-Off” or “Off-On” response from a fluorescence sensor upon binding-without binding an analyte makes it attractive sensing technique with a potential to achieve high selectivity and a detection limit of extremely low concentrations or even single molecule level.

We have successfully predicted a sensor for detecting Zn caitons that may play important roles in many physiological processes such as cellular metabolism, gene expression, apoptosis, DNA repair, Alzemeimer’s disease, diabetes, and cancer.[F1]

In the design of fluorescence sensors, a two-step computational effort was made. For a given target molecule, we first find a receptor that binds favorably with the target among candidates of receptors using molecular dynamics simulations and electronic structure calculations. Meanwhile, the absolute HOMO and LUMO energy levels are obtained for the unbound receptor and bound receptor, i.e. target-receptor.[F2] Then, we select a fluorophore by calculating its HOMO and LUMO energy levels and match the receptors. The second step is to calculate electron transfer rate using the Marcus equation and the Rehm-Weller equation.

F2. pH Sensors [F3]

Team members: Tao Lin

We have presented a DFT computational based strategy to design fluorescent sensors that exhibit PET. The frontier molecular orbitals (FMOs) of the fluorophore and electron acceptor portions of the molecule can be effectively modeled as separate units in vacuo and in solvents like water using B3LYP and 6-31G(d,p). Fluorescent quenching by electron transfer is predicted when the HOMO or LUMO of the electron acceptor lie between the FMO’s of the fluorophore. Compound 1 with a rhodamine based fluorophore and dibenzylamine acceptor exhibits reduced fluorescence at high pH and enhanced fluorescence at low pH. We are currently studying the electron transfer process in order to refine our predictions with more accurate MO calculations and also to include kinetic parameters. Future efforts will examine more complex host-guest PET systems for the detection of small carboxylic acids.[F3]

F3. Organic Molecule Sensors

Team members: George Hudson

Our current computational efforts are directed at the theoretical selection of proper fluorophore and receptor pairs that allow us to detect citrate, malate, and pyruvate using both DFT and kinetics calculations.

We have been performing calculations for designing fluorescence sensors to detect metabolites that are related to diabetes and associated problems during pregnancy.

Abstracts:

[F1] **Computational Prediction and Experimental Evaluation of a Photoinduced Electron-Transfer Sensor**

M. E. McCarroll, Y. Shi, S. Harris, S. Puli, I. Kimaru, R. Xu, L. Wang, and D. J. Dyer, J. *Phys. Chem. B* 110 (2006) 22991-22994.

An approach is presented for the design of photoinduced electron-transfer-based sensors. The approach relies on the computational and theoretical prediction of electron-transfer kinetics based on Rehm-Weller and Marcus theories. The approach allows evaluation of the photophysical behavior of a prototype fluorescent probe/sensor prior to the synthesis of the molecule. As a proof of concept, a prototype sensor for divalent metal ions is evaluated computationally, synthesized, and then analyzed spectroscopically for its fluorescence response to zinc. Calculations predicted that the system would show a competition between electron transfer and fluorescence in the free state. In the zinc-bound state, the compound was predicted to be more highly fluorescent, due to the inhibition of electron transfer. Both predictions were confirmed experimentally. A nonzero fluorescence signal was observed in the absence of zinc and an enhancement was observed in the presence of zinc. Specifically, a 56-fold enhancement was observed over a 10-fold increase in zinc concentration.

[F2] **Computational Studies on Response and Binding Selectivity of Fluorescence Sensors**

G. A. Hudson, L. Cheng, J. Yu, Y. Yan, D. J. Dyer, M. E. McCarroll, and L. Wang, *J. Phys. Chem. B* (submitted).

Using a computational strategy based on density functional theory calculations, we successfully designed a fluorescent sensor for detecting Zn^{2+} [*J. Phys. Chem. B* **2006**, *110*, 22991-22994]. In this work, we report our further studies on the computational design protocol for developing Photoinduced Electron Transfer (PET) fluorescence sensors. This protocol was applied to design a PET fluorescence sensor for Zn^{2+} ions, which consists of anthracene as the fluorophore connected to pyridine as the receptor through dimethylethanamine as the linker. B3LYP and time-dependent B3LYP calculations were performed with the basis set 6-31G(d,p), 6-31+G(d,p), 6-311G(d,p), and 6-311+G(d,p). The calculated HOMO and LUMO energies of fluorophore and receptor using all four basis sets show that the relative energy levels remain unchanged. This indicates that any of these basis sets can be used in calculating the relative molecular orbital (MO) energy levels. Furthermore, the relative MO energies of the independent fluorophore and receptor are not altered when they are linked together, which suggests that one can calculate the MO energies of these components separately and use them as the MO energies of the free sensor. These are promising outcomes for the computational design of sensors, though more case studies are needed to further confirm these conclusions. The binding selectivity studies indicate that the predicted sensor can be used for Zn^{2+} even in the presence of divalent cation, Ca^{2+}.

[F3] **Predicting Fluorescence Response in a pH Sensor by Computational Assessment of Photoinduced Electron Transfer**

R. Xu, Q. A. Best, J. Buckingham, T. Lin, M. E. McCarroll, L. Wang, and D. J. Dye, *J. Am. Chem. Soc.* (submitted).

We describe a computational strategy based on density functional theory (DFT) for the design of fluorescent sensors. The transduction mechanism of the sensors is based on photoinduced electron transfer (PET), which is predicted based on the calculated frontier molecular orbitals (FMO's). The sensor molecule is partitioned into four primary segments including the fluorophore, the electron acceptor, a binding site, and a spacer between the fluorophore and acceptor. Electron transfer is inhibited when the FMO's of the acceptor lie outside the energy gap of the fluorophore, while quenching due to electron transfer occurs when one of the acceptor FMO's lies within the energy gap for the fluorophore. A rhodamine-based pH sensor was designed and calculations in the gas phase, and in water, correctly predicted that the sensor would be highly fluorescent at low pH and PET would quench the fluorescence at high pH. The calculations utilized the B3LYP functional and it was found that acceptable results could be obtained from the smaller of two basis sets [6-31G(d,p) over 6-311G(d,p)].

Progress G

MASIS Center (**M**easurement **A**nd **S**ynthesis **I**n **S**ilico **Center**)

Team members: Tao Lin, George Hudson

Nowadays computational chemistry has been used to assist experimentalists considerably to screen synthesis routes, to measure properties of materials that are difficult to perform under normal conditions, or to understand various mechanisms. Performing such tasks, however, still relies on trained hands and minds. Thus, one of the goals in computational chemistry education is to create/provide ample opportunities for students to gain experiences on solving real problems. As such, we established the MASIS center. It is our hope that the MASIS center will help computational chemistry one step closer to achieve its goals: to become a tool that performs all the tasks in the synthesis of materials except for the final products and to replace experimental measurements.

The measurement *in silico*–performed on computer or via computer simulation–includes calorimetric measurement, IR/Raman, NMR, and even measuring mechanical properties, such as Young's Modulus. These measurements will be made by performing electronic structure calculations, mainly DFT calculations. The reaction rate calculations will mostly through kinetics and dynamics simulations.

The synthesis *in silico* currently focuses on transition metal clusters and nanoparticle. This is due to the fact that molecular dynamics simulations rely critically on the accuracy of potential energy surfaces being used. We have been engaged in constructing accurate potentials for systems consisting of transition metals. As for the synthesis of other materials, our ability is limited by the availability of potential energy surface.

So far, two projects have been carried out:

G1. Nanoparticle-Enhanced Chiral Recognition of Enantiomers [G1]

G2. Boron Isotope Separation [G2, G3]

Abstracts:

[G1] **Interparticle Chiral Recognition of Enantiomers: A Nanoparticle-Based Regulation Strategy**

I-Im S. Lim, D. Mott, M. H. Engelhard, Y. Pan, S. Kamodia, J. Luo, P. N. Njoki, S. Zhou, L. Wang, and C. J. Zhong, *Anal. Chem.* 81 (2009) 689-698.

The ability to regulate how molecular chirality of enantiomeric amino acids operates in biological systems constitutes the basis of drug design for specific targeting. We report herein a nanoparticle-based strategy to regulate interparticle chiral recognition of enantiomers using enantiomeric cysteines (L and D) and gold nanoparticles as a model system. A key element of this strategy is the creation of a nanoscale environment either favoring or not favoring the preferential configuration of the pairwise zwitterionic dimerization of the enantiomeric cysteines adsorbed on gold nanoparticles as a footprint for interparticle chiral recognition. This recognition leads to interparticle assembly of the nanoparticles which is determined by the change in the nanoparticle surface plasmonic resonance. While the surface density and functionality of cysteines on gold nanoparticles are independent of chirality, the interparticle chiral recognition is evidenced by the sharp contrast between the interparticle homochiral and heterochiral assembly rates based on a firstorder kinetic model. The structural properties for the homochiral and heterochiral assemblies of nanoparticles depend on the particle size, the cysteine chirality, and other interparticle binding conditions. The structural and thermodynamic differences between the homochiral and heterochiral interactions for the interparticle assemblies of nanoparticles were not only substantiated by spectroscopic characterizations of the adsorbed cysteine species but also supported by structures and enthalpies obtained from preliminary density functional theory calculations. The experimental-theoretical correlation between the interparticle reactivity and the enantiomeric ratio reveals that the chiral recognition is tunable by the nanoscale environment, which is a key feature of the nanoparticle-regulation strategy for the interparticle chiral recognition.

[G2] **Complex Formation between Anisole and Boron Trifluoride: Structural and Binding Properties**

T. Lin, W. Zhang, and L. Wang, *J. Phys. Chem. A* 112 (2008) 13600-13608.

The structures, energetics, and binding characteristics of complexes formed between anisole ($C_6H_5OCH_3$) and boron trifluoride (BF_3) were investigated using MP2 and B3LYP methods with 6-31+G(d,p) and 6-311+G(d,p) basis sets. Among the complexes with a 1:1 ratio of $C_6H_5OCH_3$ to BF_3, both B3LYP and MP2 methods predict the same structures and relative stability of the isomers; however, the B3LYP binding energies are smaller than the MP2 energies. Furthermore, the weaker the interaction, the greater the discrepancy in binding energy. The charge decomposition analysis (CDA) showed that there are two types of complexes: the Lewis acid-base adduct and the van der Waals complexes. The CDA results also illustrated that there is a significant donation from the oxygen lone pair electrons to the boron vacant orbital in the adduct. The van der Waals complexes were formed through the aromatic ring and BF_3 interaction or through the H and F interactions. The MP2 results showed that the formation of adduct at room temperature is thermodynamically favorable. Among the 1:2 $C_6H_5OCH_3$-BF_3 complexes, the most stable structure consists of both the Lewis acid-base and van der Waals binding; i.e., one BF_3 binds with $C_6H_5OCH_3$ to form $C_6H_5OCH_3 \cdot BF_3$ adduct, while the other BF_3 binds with this adduct through van der Waals interactions. The calculated binding energy of the 1:1 complex is close to the experimental heat of formation, which suggests that the 1:1 complexes are the most likely species in the $C_6H_5OCH_3$ and BF_3 mixture.

[G3] **Theoretical Calculation of Separation Factors for Boron Isotopic Exchange between BF_3 and $BF_3 \cdot C_6H_5OCH_3$**

T. Lin, W. Zhang, and L. Wang, *J. Phys. Chem. A* 113 (2009) 7267-7274.

The separation factors (or equilibrium constants) for boron isotopic exchange reaction $^{10}BF_3$ + $^{11}BF3 \cdot C_6H_5OCH_3 \rightleftarrows {}^{11}BF_3 + {}^{10}BF_3 \cdot C_6H_5OCH_3$ were obtained from MP2/6-31+G(d,p) and B3LYP/6-31+G(d,p) calculations. New scaling factors, single and multiple, were derived from the harmonic frequencies through the least squares fit for BF_3 and $C_6H_5OCH_3$. The use of multiple scaling factors in the case of $C_6H_5OCH_3$ led to significant improvement in the calculated frequencies over using a single scaling factor. There exists a negligible difference in the separation factors obtained by using the harmonic and the scaled frequencies of the same method, and in those obtained by using different methods. The calculated separation factors for the boron isotopic exchange reaction at 273.15, 293.15, and 298.15K are 1.039, 1.036, and 1.035, respectively, which are in excellent agreement with the experimental values, 1.041±0.002, 1.030±0.002, and 1.035±0.003. This study demonstrated the promise of using DFT (B3LYP) to obtain separation factors for the reactions where the interactions are weaker than covalent bonds but stronger than van der Waals interactions, and consequently to search for better complexation agents than $C_6H_5OCH_3$ for the isotopic separation of BF_3.

Research Publications and Presentations since August 2006

Publications:

1. G. A. Hudson, L. Cheng, J. Yu, Y. Yan, D. J. Dyer, M. E. McCarroll, L. Wang, *J. Phys. Chem. B* (submitted): "Computational Studies on Response and Binding Selectivity of Fluorescence Sensors".
2. L. Wang, T. Lin, J. I. Williams, J. Luo, P. N. Njoki, D. Mott, R. Loukrakpam, C. J. Zhong, *J. Am. Chem. Soc.* (submitted): "Optimal composition of ternary nanoparticle catalysts for oxygen reduction reaction".
3. R. Xu, Q. A. Best, J. Buckingham, T. Lin, M. E. McCarroll, L. Wang, D. J. Dyer, *J. Am. Chem. Soc.* (submitted): "Predicting fluorescence response in a pH sensor by computational assessment of photoinduced electron transfer".
4. J. Yukna, H. Tang, Jianbo Li, and L. Wang, *Phys. Rev. B* (submitted): "Theoretical studies of silver clusters".
5. W. Zhang and L. Wang, J. Phys. Chem. C (submitted): "The σ-bonds in $CH_4\cdots Pd_n$ Complexes: A Density Functional Theory Study"
6. Z. Xu, X. Shi, J. Li, S. Lu, and L. Wang, *IEEE proceedings of 2009 Fifth International Conference on Natural Computation* 1 (2009) 86-90: "Artificial neural network method to construct potential energy surfaces for transition metal nanoparticles: Pt, Au, and Ag".
7. T. Lin, W. Zhang, and L. Wang, *J. Phys. Chem. A* 113 (2009) 7267-7274: "Theoretical calculation of separation factors for boron isotopic exchange between BF_3 and $BF_3{\cdot}C_6H_5OCH_3$".
8. I-Im S. Lim, D. Mott, M. Engelhard, Y. Pan, S. Kamodia, J. Luo, P. N. Kjoki, S. Zhou, L. Wang, and C.J. Zhong, *Anal. Chem.* 81 (2009) 689-698: "Interparticle chiral recognition of enantimers: A nanoparticle-based regulation strategy".
9. T. Lin, W. Zhang, and L. Wang, *J. Phys. Chem. A* 112 (2008) 13600-13608: "Complex formation between anisole and boron trifluoride: structural and binding properties".
10. J. Yukna and L. Wang, *J. Phys. Chem. C* 111 (2007) 13337-13347: "Molecular dynamics studies of the coalescence of silver clusters".
11. L. Wang, *Chem. Phys. Lett.* 443 (2007) 304-308: "CO adsorbs upside-down on small Pt_mAu_n clusters".
12. T. Pawluk and L. Wang, *J. Phys. Chem. C* 111 (2007) 6713-6719: "Molecular dynamics simulations of the coalescence of iridium clusters".
13. T. Pawluk, L. Xiao, J. Yukna, and L. Wang, *J. Chem. Theory Comput.* 3 (2007) 328-335: "The impact of PES on MD results of the coalescence of $M_2 + M$ with M = Ir, Pt, Au, Ag".
14. L. Xiao and L. Wang, *J. Phys. Chem. B* 111 (2007) 1657-1663: "Methane activation on Pt and Pt_4: A density functional theory study".
15. M. M. Sadek and L. Wang, *J. Phys. Chem. B* 110 (2006) 14036-14042: "Effect of adsorption site, size, and composition of Pt/Au bimetallic clusters on the CO frequency: A density functional theory study".
16. M. E. McCarrol, Y. Shi, S. Harris, S. Puli, I. Kimaru, R. Xu, L. Wang, and D. J. Dyer, *J. Phys. Chem. B* 110 (2006) 22991-22994: "Computational prediction and experimental evaluation of a photoinduced electron transfer sensor".
17. K. Spivey, J. I. Williams, and L. Wang, *Chem. Phys. Lett.* 432 (2006) 163-166: "Structures of undercagold clusters: Ligand effect".
18. L. Xiao and L. Wang, *Chem. Phys. Lett.* 430 (2006) 319-322: "Density functional theory study of single-wall platinum nanotubes".

Presentations:

I. Conference presentations

1. Zhe Xu, Xiajing Shi, Jianbo Li, Susan Lu, and Lichang Wang, "Artificial neural network method to construct potential energy surfaces for transition metal nanoparticles: Pt, Au, and Ag" (talk) at *the 5th International Conference on Natural Computation*, August 14-16, 2009, Tianjin, China.

2. Lichang Wang and Minhua Zhang, “Utilization of coal: Catalysis in Direct Coal liquefaction" (invited talk) at the 2009 Forum on Clean Utilization of China Fossil Fuels, August 8-9, 2009, Beijing, China.
3. George Hudson and Lichang Wang, “DFT studies of organic dyes for use in DSSC’s” (talk) at *The 41st Midwest Theoretical Chemistry Conference*, May 28-30, 2009, Carbondale, Illinois.
4. Jianbo Li, Jennifer Yukna, Hongmei Tang, and Lichang Wang, “Theoretical studies of silver clusters” (poster) at *The 41st Midwest Theoretical Chemistry Conference*, May 28-30, 2009, Carbondale, Illinois.
5. Zhe Xu, Jianbo Li, Susuan Lu, and Lichang Wang, “Artificial neural network potential energy surface for transition metal nanoparticles: Ag” (poster) at *The 41st Midwest Theoretical Chemistry Conference*, May 28-30, 2009, Carbondale, Illinois.
6. Chasity Love and Lichang Wang, “The effect of support, ZnO, on the structure and properties of Cu clusters” (poster) at *The 41st Midwest Theoretical Chemistry Conference*, May 28-30, 2009, Carbondale, Illinois.
7. Sarah A. Ferro, Chasity B. Love, and Lichang Wang, “Transition metal clusters: DFT studies of geometrical optimization and frequencies” (poster) at *The 41st Midwest Theoretical Chemistry Conference*, May 28-30, 2009, Carbondale, Illinois.
8. Zhe Xu, Jianbo Li, Susan Lu, and Lichang Wang, “An artificial neural network potential energy surface for silver nanoparticles” (poster), at the *George C. Schatz 60th Birthday Conference*, April 17-18, 2009, Northwestern University Campus, Illinois.
9. Chasity B. Love and Lichang Wang, “Effect of ZnO on the structural and electronic properties of Cu nanoparticles” (poster) at the St. Louis Area Undergraduate Research Symposium, April 4, 2009, St. Louis Zoo, St. Louis, Missouri.
10. Sarah Ferro and Lichang Wang, “DFT studies of M_2 and M_3 clusters” (poster) at the St. Louis Area Undergraduate Research Symposium, April 4, 2009, St. Louis Zoo, St. Louis, Missouri.
11. Chasity B. Love and Lichang Wang, “The effect of support, ZnO, on the structure and properties of Cu clusters” (poster) at *The 237th National Meeting of the American Chemical Society*, March 22-26, 2009, Salt Lake City, Utah.
12. Daniel J. Dyer, Quinn Best, Ruisong Xu, George A. Hudson, Matthew McCarroll, and Lichang Wang, “Fluorescent sensor by molecular recognition and response selectivity” (talk) at *The 237th National Meeting of the American Chemical Society*, March 22-26, 2009, Salt Lake City, Utah.
13. Tao Lin, Weijiang Zhang, and Lichang Wang, “Van der Waals complexes of anisole and boron trifluoride: Structural and binding properties” (poster) at the *2008 American Conference on Theoretical Chemistry*, July 19-24, 2008, Evanston, Illinois.
14. Chasity Love and Lichang Wang, “The effect of support, ZnO, on the structure and properties of Cu clusters” (poster) at the *2008 American Conference on Theoretical Chemistry*, July 19-24, 2008, Evanston, Illinois.
15. Tiffany Pawluk and Lichang Wang, “Methane dehydrogenation on iridium clusters” (poster) at the *2008 American Conference on Theoretical Chemistry*, July 19-24, 2008, Evanston, Illinois.
16. George Hudson, Lei Cheng, Jiamei Yu, Yong Yan, Daniel J. Dyer, Matthew E. McCarroll, and Lichang wang, “Computational prediction of response and binding selectivity for photoinduced electron transfer fluorescence sensors” (poster) at the *2008 American Conference on Theoretical Chemistry*, July 19-24, 2008, Evanston, Illinois.
17. Chasity Love and Lichang Wang, “DFT studies of Cu clusters” (poster) at *The 235th National Meeting of the American Chemical Society*, April 6-10, 2008, New Orleans, Louisiana.
18. Tao Lin, Joe I. Williams, and Lichang Wang, “Why PtVFe nanoparticles are better catalysts for oxygen reduction” (talk) at *The 235th National Meeting of the American Chemical Society*, April 6-10, 2008, New Orleans, Louisiana.
19. Lichang Wang and Kasi Spivey, “Ligand induced structural phase transition of Au_{11} clusters” (poster) at *The Gordon Research Conference on Clusters, Nanaocrystals & Nanostructures*, July 29-August 3, 2007, Mount Holyoke College, South Hadley, MA.

20. Chasity B. Love and Lichang Wang, "Comparative DFT studies of small Cu clusters" (poster) at *The 39th Midwest theoretical chemistry conference*, June 28-30, 2007, Indiana University, Bloomington, Indiana.
21. Tiffany Pawluk and Lichang Wang, "DFT studies of methane dehydrogenation on Ir atoms" (poster) at *The 39th Midwest theoretical chemistry conference*, June 28-30, 2007, Indiana University, Bloomington, Indiana.
22. Tiffany Pawluk and Lichang Wang, "Molecular dynamics simulations of the coalescence of iridium clusters" (poster) at *The 233rd National Meeting of the American Chemical Society*, March 25-29, 2007, Chicago, Illinois.
23. Mark M. Sadek and Lichang Wang, "DFT study of the CO adsorption on Pt/Au bimetallic clusters" (poster) at *The 233rd National Meeting of the American Chemical Society*, March 25-29, 2007, Chicago, Illinois.
24. Joe I. Williams and Lichang Wang, "O_2 chemisorption on PtVFe Nanoparticles: A Density Functional Theory Study" (poster) at *The 233rd National Meeting of the American Chemical Society*, March 25-29, 2007, Chicago, Illinois.
25. Daniel J. Dyer, Ruisong Xu, Irene Kimaru, Charles Cook, Lichang Wang, and Matthew E. McCarroll, "Response-selective fluorescent sensors based on molecular recognition" (talk) at *The 233rd National Meeting of the American Chemical Society*, March 25-29, 2007, Chicago, Illinois.
26. L. Wang, T. Pawluk, L. Xiao, and J. Yukna, "Molecular dynamics simulation on the coalescence of Pt, Ir, Au, and Ag clusters" (talk) at *The 232nd National Meeting of the American Chemical Society*, September 9-15, 2006, San Francisco, California.

II. Department/Institution seminars

1. Lichang Wang, R & D Center for Petrochemical Technology, Tianjin University, August 13, 2009: "Photon-Electron Transfer and the Application of Coal in Solar Cells".
2. Lichang Wang, Department of Chemistry, Tennessee State University, February 7, 2008: "Using Computational Chemistry to Study Catalyst Nanoparticles for Fuel Cell Reactions".
3. Lichang Wang, Department of Chemistry, The Ohio State University, October 22, 2007: "Insight into catalyst nanoparticles for fuel cell reactions via computational chemistry".
4. Lichang Wang, Department of Chemistry, Beijing University, June 22, 2007: "Computational modeling in uncovering the uniqueness of transition metal clusters".
5. Lichang Wang, Institute of Chemical Engineering, Tianjin University, June 21, 2007: "Computational modeling in uncovering the uniqueness of transition metal nanoparticles".

Support since August 2006

We are grateful for the support from:

- NSF-NCSA computing resources (Che090073, 4/22/09–4/16/10)
- China Scholarship Council (1/28/09–1/27/13)
- NIH (1R15GM080721-01A1, 2/1/08–1/31/10)
- China Scholarship Council (9/17/07–9/16/08)
- NSF (CBET-0709113, 9/1/07–8/31/11)
- SIU-UGA (8/20/07–5/9/08)
- NSF-REU (DMR-0552800, 7/1/07–4/30/12)
- ACS-PRF (41572-G5, 7/1/04–8/31/07)